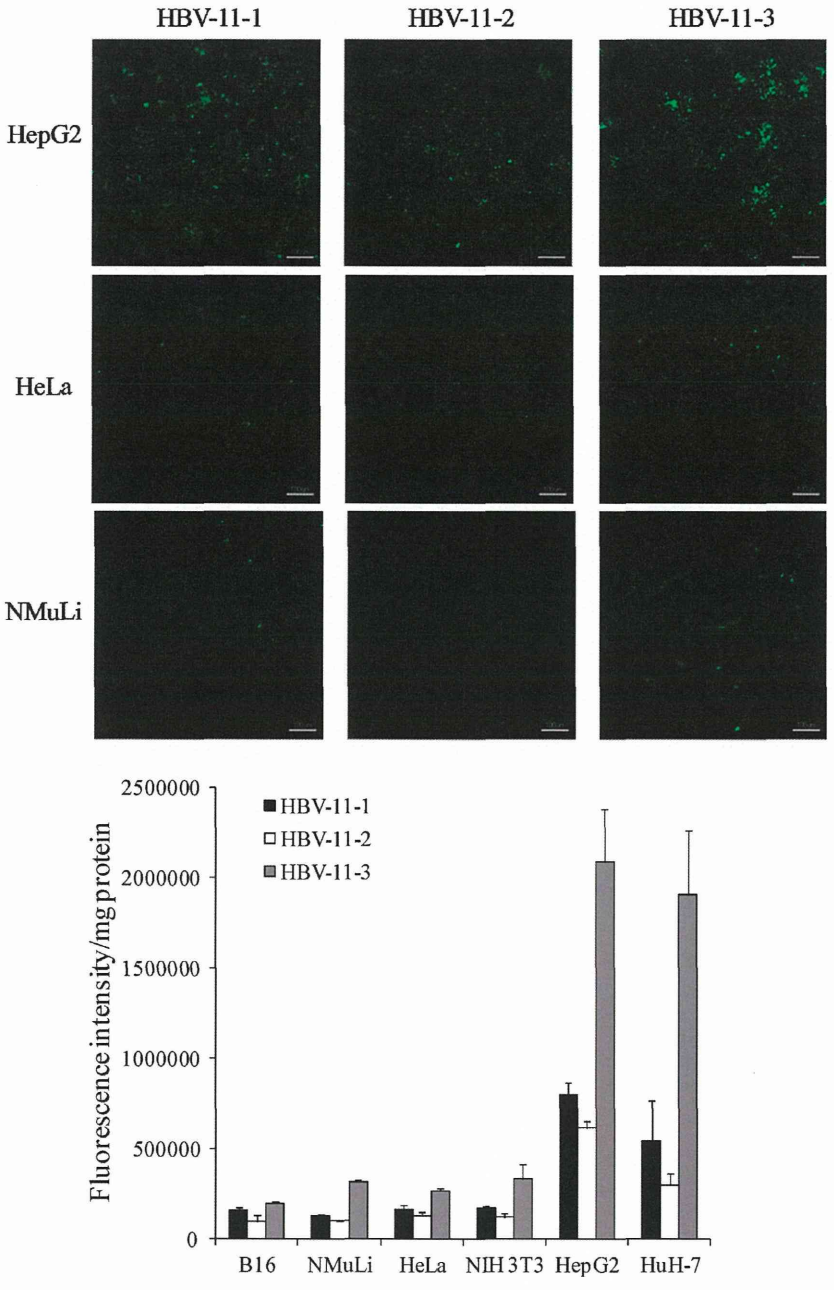

Fig. 3. Peptide binding selectivity for each cell line. FITC-labeled fluorescent peptides were added to each cell and fluorescence intensities were determined. The fluorescence levels are presented as fluorescence intensity/mg total protein.

Acknowledgments

This work was financially supported by a grant-in-aid for Scientific Research (B) (KAKENHI Grant Number 23310085) from the Ministry of Education, Culture, Sports, Science and Technology (MEXT) of Japan.

Appendix A. Supplementary data

Supplementary material related to this article can be found, in the online version, at http://dx.doi.org/10.1016/j.jviromet.2014.02.013.

References

Bremer, C.M., Sominskaya, I., Skrastina, D., Pumpens, P., El Wahed, A.A., Beutling, U., Frank, R., Fritz, H.J., Hunsmann, G., Gerlich, W.H., Glebe, D., 2011. N-terminal myristoylation-dependent masking of neutralizing epitopes in the preS1 attachment site of hepatitis B virus. J. Hepatol. 55, 29–37.

Engelke, M., Mills, K., Seitz, S., Simon, P., Gripon, P., Schnölzer, M., Urban, S., 2006. Characterization of a hepatitis B and hepatitis delta virus receptor binding site. Hepatology 43, 750–760.

Glebe, D., Urban, S., 2007. Viral and cellular determinants involved in hepadnaviral entry. World J. Gastroenterol. 13, 22–38.

Glebe, D., Urban, S., Knoop, E.V., Çağ, N., Krass, P., Grün, S., Bulavaite, A., Sasnauskas, K., Gerlich, W.H., 2005. Mapping of the hepatitis B virus attachment site by use of infection-inhibiting preS1 lipopeptides and tupaia hepatocytes. Gastroenterology 129, 234–245.

Gripon, P., Cannie, I., Urban, S., 2005. Efficient inhibition of hepatitis B virus infection by acylated peptides derived from the large viral surface protein. J. Virol. 79, 1613–1622.

Hu, W.G., Wei, J., Xia, H.C., Yang, X.X., Li, F., Li, G.D., Wang, Y., Zhang, Z.C., 2005. Identification of the immunogenic domains in HBsAg preS1 region using overlapping preS1 fragment fusion proteins. World J. Gastroenterol. 11, 2088–2094.

Kang, J.H., Oishi, J., Kim, J.H., Ijuin, M., Toita, R., Jun, B., Asai, D., Mori, T., Niidome, T., Tanizawa, K., Kuroda, S., Katayama, Y., 2010. Hepatoma-targeted gene delivery using a tumor cell-specific gene regulation system combined with a human liver cell-specific bionanocapsule. Nanomed.: Nanotechnol. Biol. Med. 6, 583–589.

Lee, K.W., Tey, B.T., Ho, K.L., Tan, W.S., 2012. Delivery of chimeric hepatitis B core particles into liver cells. J. Appl. Microbiol. 112, 119–131.

Mahtab, M.A., Rhman, S., Khan, M., Karim, F., 2008. Hepatitis B virus genotypes: an overview. Hepatobiliary Pancreat. Dis. Int. 7, 457–464.

McMahon, B.J., 2009. The influence of hepatitis B virus genotype and subgenotype on the natural history of chronic hepatitis B. Hepatol. Int. 3, 334–342.

Meier, A., Mehrle, S., Weiss, T.S., Mier, W., Urban, S., 2013. Myristoylated preS1-domain of the hepatitis B virus L-protein mediates specific binding to differentiated hepatocytes. Hepatology 58, 31–42.

Miyata, R., Ueda, M., Jinno, H., Konno, T., Ishihara, K., Ando, N., Kitagawa, Y., 2009. Selective targeting by preS1 domain of hepatitis B surface antigen conjugated with phosphorylcholine-based amphiphilic block copolymer micelles as a biocompatible, drug delivery carrier for treatment of human hepatocellular carcinoma with paclitaxel. Int. J. Cancer 124, 2460–2467.

Murata, M., Narahara, S., Umezaki, K., Toita, R., Tabata, S., Piao, J.S., Abe, K., Kang, J.H., Oouchida, K., Cui, L., Hashizume, M., 2012. Liver cell specific targeting by the preS1 domain of hapatitis B virus surface antigen displayed on protein nanocages. Int. J. Nanomed. 7, 4353–4362.

Seeger, C., Mason, W.S., 2000. Hepatitis B virus biology. Microbiol. Mol. Biol. Rev. 64, 51–68.

Zhang, X., Lin, S.M., Chen, T.Y., Liu, M., Ye, F., Chen, Y.R., Shi, L., He, Y.L., Wu, L.X., Zheng, S.Q., Zhao, Y.R., Zhang, S.L., 2011. Asialoglycoprotein receptor interacts with the preS1 domain of hepatitis B virus *in vivo* and *in vitro*. Arch. Virol. 156, 637–645.

Journal of Gastroenterology and Hepatology

JGHF

doi:10.1111/jgh.12893

HEPATOLOGY

Basic fibroblast growth factor-treated adipose tissue-derived mesenchymal stem cell infusion to ameliorate liver cirrhosis via paracrine hepatocyte growth factor

Wei-Ping Tang,* Tomohiko Akahoshi,*,† Jing-Shu Piao,* Sayoko Narahara,* Masaharu Murata,* Takahito Kawano,* Nobuhito Hamano,* Tetsuo Ikeda† and Makoto Hashizume*

*Department of Disaster and Emergency Medicine, Faculty of Medicine, and †Department of Surgery and Science, Graduate School of Medical Sciences, Kyushu University, Fukuoka, Japan

Key words
ADSCs, bFGF, HGF, liver cirrhosis, RNA interference.

Accepted for publication 20 December 2014.

Correspondence
Dr. Tomohiko Akahoshi, Department of Disaster and Emergency Medicine, Faculty of Medicine, Kyushu University, 3-1-1 Maidashi, Higashi-ku, Fukuoka 812-8582, Japan. Email: tomohiko@surg2.med.kyushu-u.ac.jp

Disclosure: The authors report no potential conflict of interest in this work.

Abstract

Background and Aim: Recent studies show that adipose tissue-derived mesenchymal stem cells have potential clinical applications. However, the mechanism has not been fully elucidated yet. Here, we investigated the effect of basic fibroblast growth factor-treated adipose tissue-derived mesenchymal stem cells infusion on a liver fibrosis rat model and elucidated the underlying mechanism.

Methods: Adipose tissue-derived mesenchymal stem cells were infused into carbon tetrachloride-induced hepatic fibrosis rats through caudal vein. Liver functions and pathological changes were assessed. A co-culture model was used to clarify the potential mechanism.

Results: Basic fibroblast growth factor treatment markedly improved the proliferation, differentiation, and hepatocyte growth factor expression ability of adipose tissue-derived mesenchymal stem cells. Although adipose tissue-derived mesenchymal stem cells infusion alone slightly ameliorated liver functions and suppressed fibrosis progression, basic fibroblast growth factor-treatment significantly enhanced the therapeutic effect in association with elevated hepatocyte growth factor expression. Moreover, double immunofluorescence staining confirmed that the infused cells located in fibrosis area. Furthermore, co-culture with adipose tissue-derived mesenchymal stem cell led to induction of hepatic stellate cell apoptosis and enhanced hepatocyte proliferation. However, these effects were significantly weakened by knockdown of hepatocyte growth factor. Mechanism investigation revealed that co-culture with adipose tissue-derived mesenchymal stem cells activated c-jun N-terminal kinase-p53 signaling in hepatic stellate cell and promoted apoptosis.

Conclusions: Basic fibroblast growth factor treatment enhanced the therapeutic effect of adipose tissue-derived mesenchymal stem cells, and secretion of hepatocyte growth factor from adipose tissue-derived mesenchymal stem cells plays a critical role in amelioration of liver injury and regression of fibrosis.

Introduction

Liver cirrhosis is characterized by parenchymal fibrosis associated with liver dysfunction.[1–3] There is no effective therapy apart from liver transplantation. Recent stem cell therapies have progressed significantly.[4–6] Of these approaches, bone marrow cells have been reported as an effective therapeutic agent for hepatitis patients.[7,8] However, it is difficult to obtain bone marrow cells because of painful procedures and relatively low cell yields.[9] Therefore, a cell source with an easier approach for isolation is desirable for cell therapy. Adipose tissue-derived mesenchymal stem cells (ADSCs) are an attractive cell source for regenerative medicine because of their multipotency.[10,11] ADSCs can differentiate into multiple lineages such as hepatocytes and blood vessels.[12,13] Compared with bone marrow cells, ADSCs can be easily obtained in large numbers by minimally invasive methods and show better immunocompatibility.[14] Moreover, there are increasing studies of the ability of ADSCs to mediate anti-inflammatory and healing effects via paracrine cytokines such as hepatocyte growth factor (HGF) and vascular endothelial growth factor.[15,16] However, the underlying mechanism of the antifibrotic effect of ADSCs is largely unknown.

In the present study, we hypothesized that bFGF-treated ADSC infusion may enhance the amelioration of liver fibrogenesis and the recovery of liver dysfunction in a carbon tetrachloride (CCl_4)-induced cirrhosis rat model via overexpressing HGF. To test this hypothesis, we infused ADSCs into hepatic cirrhosis rats and confirmed their homing by bio-fluorescence imaging and double immunofluorescence staining. Furthermore, a co-culture model

was employed to investigate the influence of ADSCs on hepatic stellate cells (HSCs) and hepatocytes, and elucidate the underlying mechanism. Moreover, to identify the role of HGF, we transfected ADSCs with HGF siRNA followed by co-culture with HSCs or hepatocytes.

Methods

ADSC preparation and characteristics. Six-week-old male Fischer 344 rats (Charles River, Atsugi, Japan) were housed under controlled temperature, humidity, and lighting conditions. The study was approved by the Committee of Animal Experiment Ethics at Kyushu University. All procedures were carried out in strict accordance with the approved experimental plan.

Rat ADSCs were collected from the inguinal fat pad.[17] Briefly, adipose tissues were minced, digested in 1 mg/mL collagenase (Sigma-Aldrich, St. Louis, Germany), filtered through a 70-μm nylon filter (BD Biosciences, San Diego, USA), and then cultured in Dulbecco's modified Eagle's medium containing 10% fetal bovine serum (FBS; Gibco, Carlsbad, CA, USA), 10 ng/mL bFGF (Wako, Tokyo, Japan), and antibiotic-antimycotic (Gibco). Passage three to five cells were used.

For the cell proliferation assay, ADSCs were seeded in 24-well plates in the presence or absence of bFGF, and cell numbers were counted at 8 and 72 h of incubation using a cell counter (Bio-Rad, Hercules, CA, USA). For the DNA synthesis assay, ADSCs were seeded in six-well u-slide (Ibidi, Munich, Germany) and analyzed using a Click-iT EdU Image Kit (Invitrogen, Carlsbad, CA, USA). The cells were immunostained with anti-HGF antibody (Santa Cruz, Heidelberg, Germany) and then fluorescein isothiocyanate (FITC)-conjugated secondary antibody (Sigma-Aldrich). EdU-positive cells were counted and compared with total cell counts. Proliferation rates were calculated from two independent experiments in duplicate.

Adipogenic differentiation was induced with an adipogenesis differentiation kit (Invitrogen) for 10 days and assessed by Oil-Red-O (Sigma-Aldrich) staining. Chondrogenic differentiation was induced with a chondrogenesis differentiation kit (Invitrogen) for 2 weeks, and then, the cells were stained with 1% Alcian Blue (Sigma-Aldrich). Cell immunophenotypes were analyzed by flow cytometer (BD Biosciences). Briefly, cells were incubated with fluorescein-coupled antibodies against CD29, CD44, CD90, or CD45 (BD Biosciences). Appropriate antibody isotypes were used as negative controls.

Experimental protocol. Rats were randomly divided into four groups with 10 rats in each group: A (three times ADSC infusion + CCl_4); B (one time ADSC infusion + CCl_4); C (ADSC [bFGF-] infusion + CCl_4); D (PBS + CCl_4). Hepatic cirrhosis was induced by intraperitoneal injection of 1 mg/kg body weight CCl_4 (Wako) twice a week for 8 weeks.[18] Then, 5×10^6 PKH26 (Sigma-Aldrich)- or Qtracker705 nanoparticle (Invitrogen)-labeled ADSCs in 0.5 mL PBS were infused via the caudal vein. Rats infused with 0.5-mL PBS were used as controls. Three days after infusion, the rats were sacrificed and exsanguinated to test serum levels of alanine transaminase (ALT), aspartate aminotransferase (AST), and albumin (ALB). Tissues were collected for *ex vivo* imaging analysis and histological examination.

Liver histology. Masson trichrome staining was performed to examine collagen matrix deposition in livers. To calculate the percentage of the blue-stained fibrotic area, five random fields per section were assessed by two observers with Adobe Photoshop (Adobe Inc. San Jose, CA, USA) and Image J (NIH, Bethesda, MD, USA) in a blinded manner. Next, we performed double immunofluorescence staining of HGF and PKH26 in liver sections. Briefly, tissues were incubated sequentially with the anti-HGF antibody and secondary antibody, and then mounted in Vectashield medium (Vector, Burlingame, CA, USA). Unlabeled ADSC-infused liver sections served as negative controls.

Western blot analysis. Total protein (40 μg) from liver samples or cell lysates was loaded and separated in a sodium dodecyl sulfate polyacrylamide gel electrophoresis gel (Invitrogen) and then transferred to a membrane (Millipore, Temecula, CA, USA). Membranes were blocked and then incubated sequentially with primary antibodies and appropriate secondary antibodies. Primary antibodies were as follows: HGF, proliferating cell nuclear antigen (PCNA), ALB (Santa Cruz); α-smooth muscle actin (α-SMA), β-actin (Sigma-Aldrich); and c-jun N-terminal kinase (JNK) 1/2, phospho-JNK1/2, extracellular signal-regulated kinase (ErK)1/2, phospho-ErK1/2, p53, and phospho-p53 (Cell Signaling, USA).

Ex vivo fluorescence imaging assay. ADSCs were labeled by a Qtracker705 cell labeling kit (Invitrogen) according to the manufacturer's instructions. To monitor *in vivo* distribution of ADSCs, Qtracker705-labeled ADSCs were infused, whereas unlabeled ADSC-infused rats served as negative controls to adjust for the influence of auto-fluorescence. Further confirmation was obtained by performing *ex vivo* bio-fluorescence imaging using an IVIS Spectrum imaging system (Xenogen, Alameda, CA, USA) at 3 days after ADSC infusion.

Transfection of ADSCs with HGF siRNA. ADSCs were cultured in OPTI-MEM/5% FBS (Invitrogen) with or without bFGF. At 60% confluence, ADSCs were transfected for 48 h with Silencer select HGF siRNA or negative control siRNA (Applied Biosystems, Foster City, CA, USA) using Lipofectamine RNAiMAX (Invitrogen). Conditioned medium was assayed using a HGF Quantikine ELISA Kit (R&D Systems, Minneapolis, MN, USA). For quantitative real-time polymerase chain reaction (PCR) or reverse-transcription (RT)-PCR, total RNA was extracted using an RNeasy Plus Mini Kit (Qiagen, Hilden, Germany) and analyzed using iTaq universal SYBR green one-step kit (Bio-rad) or SuperScript III one-step RT-PCR system (Invitrogen). Primers used were HGF (NM_017017.2), hepatocyte nuclear factor 4 alpha (NM_001270933), and GAPDH (NM_017008.4) (Takara, Japan).

Primary liver cell isolation and co-culture assay. Primary rat hepatocytes were obtained by collagenase perfusion and purified by iodixanol density solution (OptiPrep, Axis-shield, Oslo, Norway) as described previously.[19] Hepatocytes obtained from normal liver were seeded on collagen-coated coverslips (BD

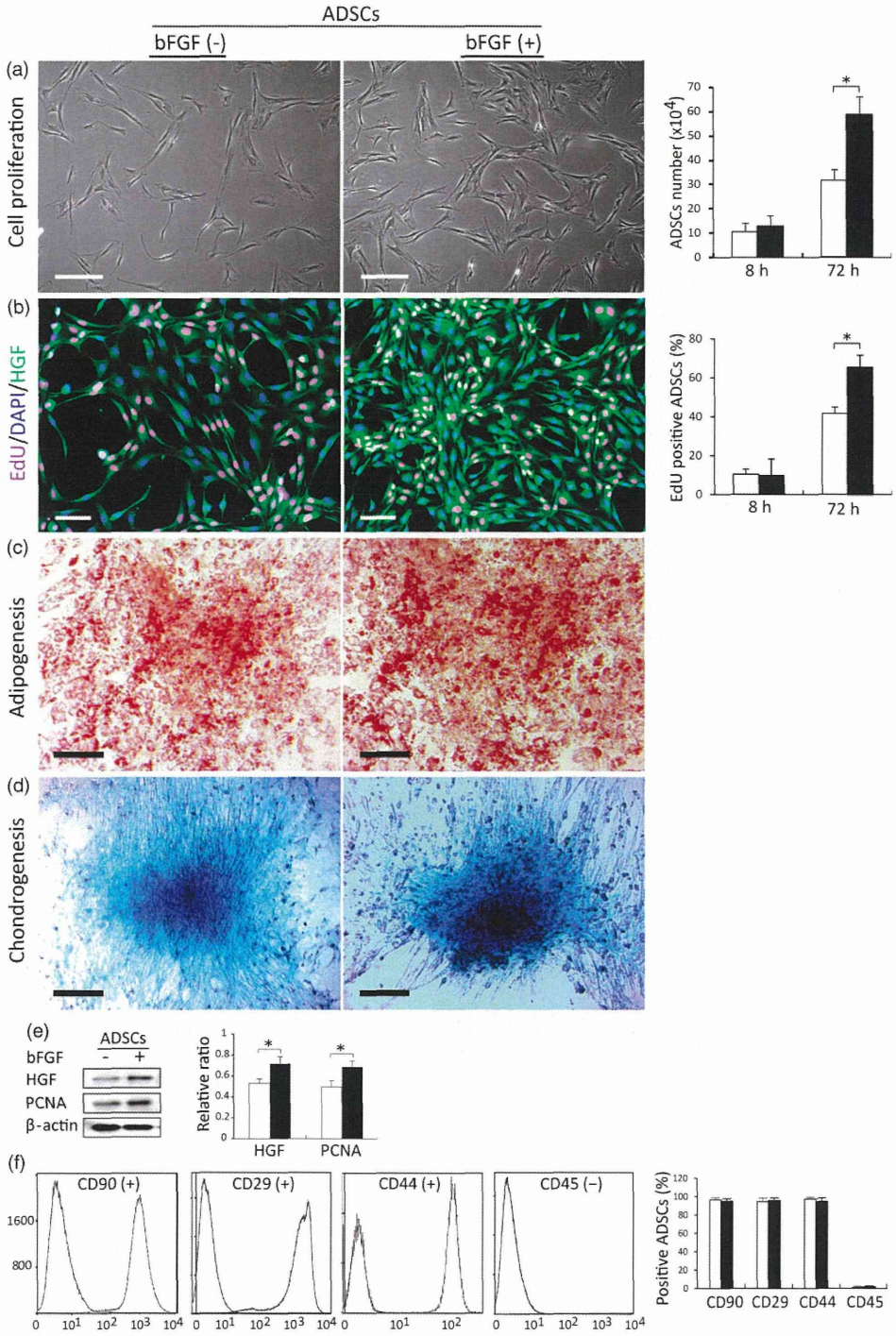

Figure 1 Basic fibroblast growth factor (bFGF) treatment enhances the pluripotent ability of adipose tissue-derived mesenchymal stem cells (ADSCs). (a) Phase contrast image of ADSCs expanded in complete medium in the presence or absence of bFGF. (b) Cell proliferation assessed by EdU endocytosis assay. (c) In the presence or absence of bFGF, ADSCs differentiated into adipocytes as indicated by intracellular accumulation of lipid vesicles (red, Oil Red O). (d) Under chondrogenic induction, ADSCs produced proteoglycans (blue, Alcian Blue). (e) Western blot analyses of hepatocyte growth factor (HGF) and proliferating cell nuclear antigen (PCNA) expression by ADSCs in the presence or absence of bFGF for 3 days. (f) Flow cytometric analysis of ADSC immunophenotypes. Cells were stained with Immunoglobulin G (IgG) isotype-matched control antibodies or antibodies against CD90, CD29, CD44, or CD45. Scale bar = 20 μm. □, bFGF (–); ■, bFGF (+).

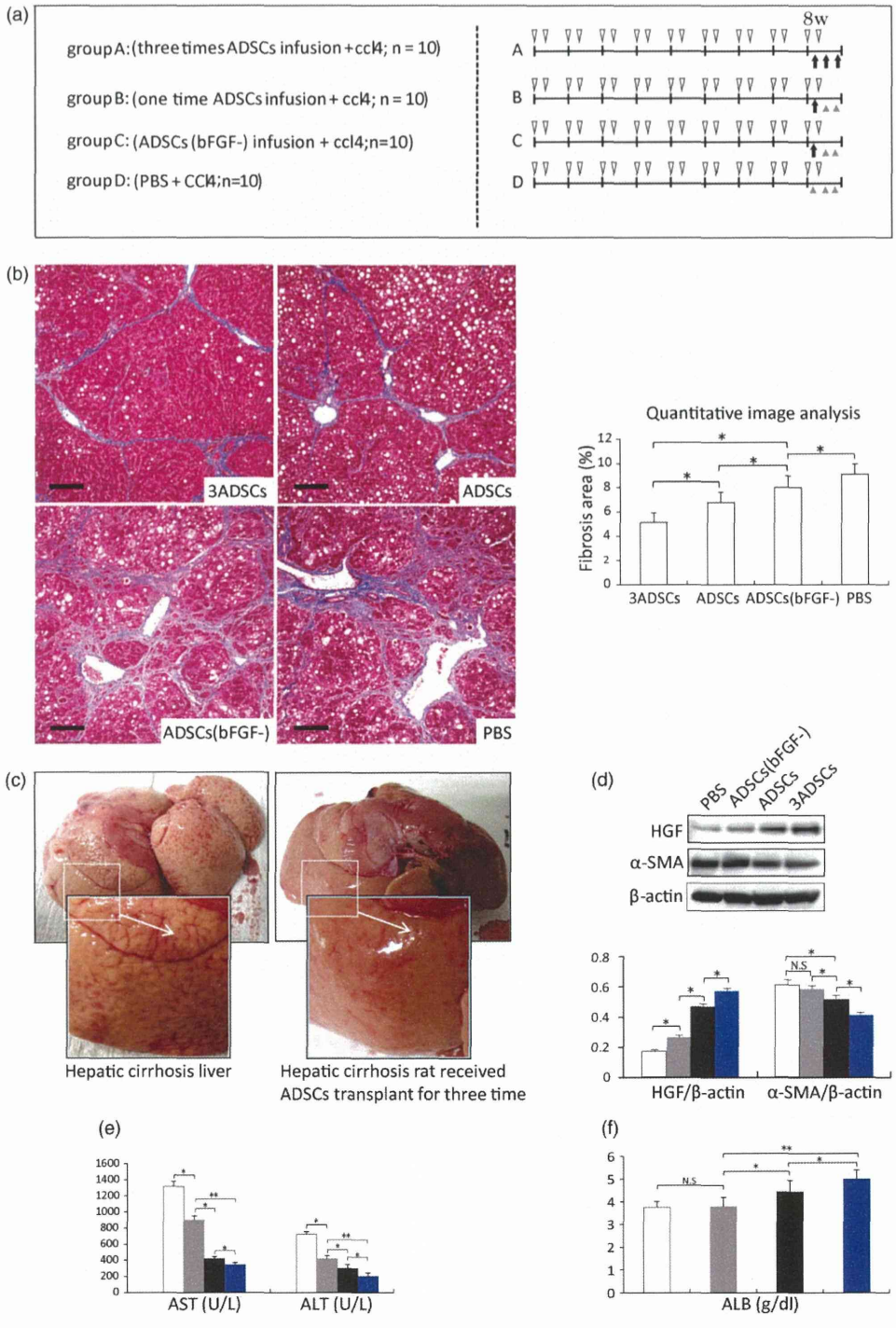

Figure 2 Experimental protocol and effects of adipose tissue-derived mesenchymal stem cell (ADSC) infusion on hepatic cirrhosis. (a) Rat models: group A (three times ADSC infusion + carbon tetrachloride [CCl4]); group B (one time ADSC infusion + CCl4); group C [ADSC (bFGF-) infusion + CCl4]; group D (phosphate-buffered saline [PBS] + CCl4). Experimental protocol: CCl4 was administered by intraperitoneal injection at a dose of 1 mg/kg twice a week for 8 weeks; then, ADSCs were infused via the caudal vein. Changes in the severity of liver fibrosis were investigated at 3 days after ADSC infusion. (b) Representative images and quantitative analysis of fibrosis by Masson trichrome staining. Scale bar = 50 μm. (c) Macroscopic changes of ADSC-infused liver tissue. (d) Western blot analysis of hepatocyte growth factor (HGF) and α-SMA in liver tissue. β-Actin was used as an internal control. The intensity of each target protein was normalized to that of β-actin. (e) Serum ALT and AST levels, and the (f) serum ALB level in liver-injured rats treated with or without ADSCs. ▽, ccl4 i.p.; ↑, ADSCs iv; ▲, PBS iv; □, PBS; ■, ADSCs(bFGF-); ■, ADSCs; ■, 3ADSCs.

Biosciences). Then, HSCs in supernatants were purified by 11.5% and 16% iodixanol density gradient centrifugation.[20] Passage one to three HSCs were used.

In co-culture experiments, 1×10^4 ADSCs were plated in the upper chamber of a cell culture insert (1-μm pore size, BD Biosciences) and co-cultured with either 1×10^5 HSCs or hepatocytes on coverslips in the bottom chamber. In parallel, cells cultured alone served as controls. Cell proliferation and apoptosis were analyzed after 3 days of culture. HSC and hepatocyte proliferation were assessed by EdU endocytosis assay as just described. Cells were also incubated sequentially with anti-α-SMA or -ALB antibodies (Santa Cruz, USA) and FITC-conjugated secondary antibodies.

The apoptosis assay was conducted by flow cytometric analysis of HSCs stained with Alexa Fluor 488-conjugated annexin V and propidium iodide (PI) (Invitrogen). Early apoptotic HSCs were annexin V+/PI–, and late apoptotic HSCs were annexin V+/PI+. Furthermore, caspase-3/7 activity in HSCs was assessed using Caspase-3/7 reagent (Essen Bioscience, Tokyo, Japan). Cells were counterstained with an aSMA-Cy3 antibody (Sigma-Aldrich). To confirm p-JNK expression, HSCs were immunostained for p-JNK.

Statistical analyses. Results are presented as means ± standard deviation. The Mann–Whitney *U* test was used to detect the statistical significance between two groups. Comparisons between multiple groups were made using the Kruskal–Wallis test. A value of $P < 0.05$ was considered statistically significant.

Results

bFGF facilitates the proliferation, differentiation, and HGF expression of ADSCs. In the presence of bFGF, we found a higher proliferation rate (Fig. 1a,b) and an increased fluorescence intensity of HGF (green) in ADSCs (Fig. 1b). Moreover, adipogenic and chondrogenic differentiation abilities were enhanced (Fig. 1c,d). Western blotting confirmed that HGF and PCNA expression was significantly elevated in the presence of bFGF (Fig. 1e). Furthermore, flow cytometric analysis revealed that the cells were positive for typical mesenchymal stem cell-associated markers such as CD29, CD44, and CD90 (Fig. 1f). In other way, bFGF treatment did not have significant influence on surface marker (Fig. 1f). These data further validated the notion that bFGF is critical for self-renewal of ADSCs.[21]

bFGF -treatment enhances attenuation of hepatic fibrosis and recovery of liver functions. The experimental protocol is illustrated in Figure 2a. After 8 weeks of continuous CCl_4 administration, the liver showed typical histological changes indicating necrosis of parenchymal cells, vacuolar degeneration, and collagen deposition. Rats that received bFGF-treated ADSC infusion (groups A and B) still showed visible liver injury (Fig. 2b). However, compared with rats treated with PBS alone, histological examination revealed a significant reduction of the fibrotic area (Fig. 2b), despite a slight reduction of fibrosis in the ADSC (bFGF-) group. Furthermore, an obvious macromorphological change was observed in ADSC-infused livers (Fig. 2c). The difference between group B and C indicated that bFGF treatment further enhanced the antifibrotic effect of ADSCs. Compared with the untreated ADSC group, Western blotting showed that HGF expression was increased more significantly, and α-SMA expression was decreased in the bFGF-treated ADSC group (Fig. 2d). These results indicated that elevated HGF expression may be involved in the enhanced effects of bFGF-treated ADSCs.

Liver injury parameters such as serum ALT and AST levels were markedly increased after CCl_4 administration (~16-fold increase in ALT levels and ~15.7-fold increase in AST levels compared with

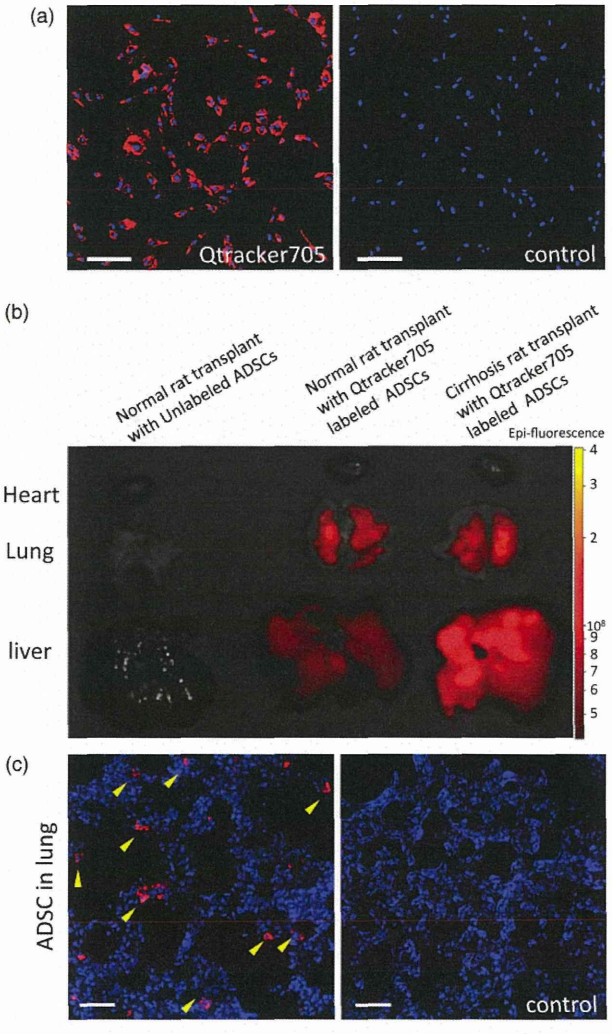

Figure 3 Fluorescent tracing of infused adipose tissue-derived mesenchymal stem cells (ADSCs). (a) Detection of Qtracker705-labeled ADSCs by fluorescence microscopy. Unlabeled ADSCs were used as a negative control. (b) ADSC engraftment monitored by *ex vivo* fluorescence imaging. Rats received infusion of Qtracker705-labeled or unlabeled ADSCs then sacrificed for organ examinations at 3 days after ADSC infusion. Red–yellow fluorescence was detected in the liver and lung. All imaging experiments were performed under the same conditions. (c) ADSCs were detected in the lung (indicated by yellow arrowheads). Scale bar = 50 μm.

those in normal rats; data not shown). In the ADSC (bFGF-) group, ALT and AST levels were significantly lower than those in the PBS group and further reduced in the bFGF-treated ADSC group. In addition, rats that underwent bFGF-treated ADSC infusion showed a gradual increase in ALB levels (Fig. 3b). More importantly, the ALB level was elevated further by three time infusions of bFGF-treated ADSCs. AST and ALT levels in rats infused three times with bFGF-treated ADSCs were notably decreased even more. However, there were no significant difference in ALB levels between ADSC alone and PBS groups. Taken together with the potent promotion of the proliferation and HGF expression ability of ADSCs by bFGF, these findings strengthened that bFGF

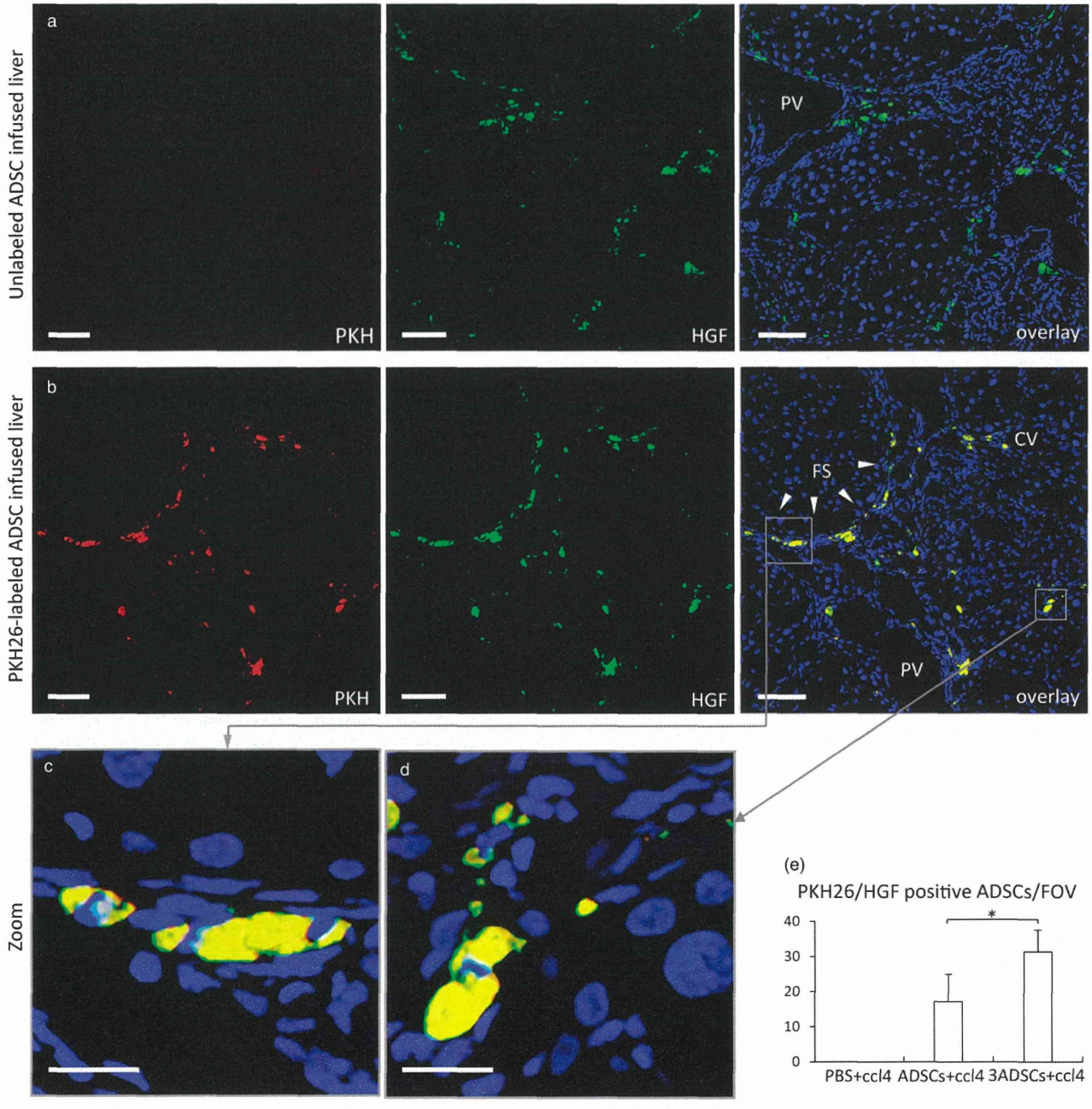

Figure 4 Immunofluorescence analysis of hepatocyte growth factor (HGF) expression in vivo. (a) Unlabeled adipose tissue-derived mesenchymal stem cell (ADSC)-infused liver section were used as control. (b) Expression of HGF (green) after PKH26 (red)-labeled ADSC infusion. Yellow indicates PKH26/HGF double-positive ADSCs. (c) ADSCs along fibrous areas. (d) ADSCs in the parenchyma. (e) Quantitative analysis of double-positive cells in the liver. Data are the means ± SD. $*P < 0.05$. PV, portal vein; CV, central vein; FS, fibrotic septa. Scale bars = 50 μm (a,b) and 20 μm (c,d).

treatment is beneficial for the biological and therapeutic effects of ADSCs.

Infused ADSCs engraft in the injured liver. Fluorescence images showed that most of Qtracker705 nanoparticles were incorporated into ADSCs, indicating a high incorporation efficiency (Fig. 3a). To track the *in vivo* distribution of ADSCs, fluorescent signals from livers were examined by *ex vivo* imaging analysis. Compared with normal liver, a significantly higher fluorescence signal from cirrhotic liver indicated promotion of infused ADSC migration into the injured site, despite a small proportion of ADSCs were trapped in the lung (Fig. 3b,c). Our data suggest that intravenously infused ADSCs have the potential to migrate into normal and injured livers, particularly under the conditions of liver damage.

The auto-fluorescence of the integrated cells were too faint to be detected, and no significant difference was found between the auto-fluorescence signal from the integrated ADSCs and parenchymal cells (Fig. 4a). In contrast, significant PKH26-HGF fluorescence signals were detected in PKH26-labeled ADSC-infused livers. As shown in Figure 4b–d, numerous ADSCs were localized along collagen fibers, parenchyma, and portal tracts, further confirmed that the infused ADSCs migrated to the injury site. Moreover, double-positive yellow cells with a stretching morphology were observed in ADSC-infused livers, indicating that the ADSCs were still viable and express HGF efficiency *in vivo*. Quantitative analysis revealed more ADSCs in livers when infused three times (Fig. 4d). These results suggested that HGF may be involved in ADSC recruitment to the liver. These data are consistent with previous reports that HGF is an important regulator of cell migration.[22]

Quantitative analysis of HGF expression and knockdown efficiency. Next, we determined the amount of HGF in ADSC-conditioned medium. A total of 2×10^5 ADSCs were cultured for 72 h, resulting in secretion of 2137.2 ± 261.5 pg/mL HGF (Fig. 5b). In addition, bFGF stimulation significantly enhanced the secretion of HGF to 4776.2 ± 532.4 pg/mL, indicating that ADSCs are sensitive to bFGF stimulation and up-regulate HGF expression efficiently. Transfection of ADSCs with HGF siRNA partially abrogated the effects of bFGF on both mRNA (Fig. 5a) and protein (Fig. 5b) levels.

ADSCs enhance hepatocyte proliferation but suppress HSC survival via HGF. When co-cultured with ADSCs, hepatocytes showed a higher efficiency for DNA synthesis even without significant engraftment (Fig. 6a). For co-cultured HSCs, we found a decrease in the DNA synthesis rate (~7%, Fig. 6b) but a significant increase in the apoptosis rate as indicated by caspase-3/7 staining (~9%, Fig. 6c) and flow cytometry analysis (~8%, Fig. 6d). We transfected ADSCs with HGF siRNA to identify whether HGF mediated the effects of ADSCs. Importantly, the observed effects were abrogated by downregulation of HGF expression (Fig. 6a–d). Collectively, these results further confirmed that paracrine HGF is critical for the effect of ADSC on HSC and hepatocyte.

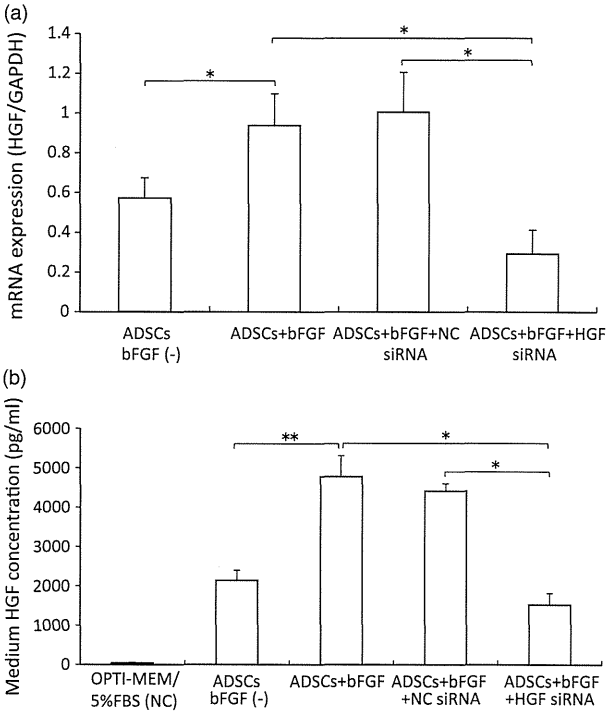

Figure 5 Analysis of hepatocyte growth factor (HGF) expression in adipose tissue-derived mesenchymal stem cells (ADSCs). (a) HGF mRNA expression and knockdown efficiency in ADSCs was quantified by real-time-PCR. (b) Analysis of HGF protein levels in conditioned medium by ELISA. HGF expression was about twofold higher in basic fibroblast growth factor (bFGF)-treated ADSCs than that in untreated ADSCs.

We next investigated whether the JNK pathway was involved in ADSC-induced HSC apoptosis. Western blot analysis showed that co-culture with ADSC did not have significant effect on activation of ErK which was involved in the prevention of apoptosis. However, expression of p-JNK in HSCs was increased significantly (Fig. 6e,f), and its downstream molecule p53 was phosphorylated as well, followed by activation of the effector caspase-3 (Fig. 6c), which induced HSC apoptosis and inhibited αSMA expression (Fig. 6e). These results suggested that ADSC-induced HSC apoptosis was involved in activation of JNK and p53 signaling but did not significantly affect ErK activity. Taken together with the results of HGF RNA interference experiments, HGF from ADSCs may contribute to the inhibitory effects on HSCs. These findings are consistent with a previous study demonstrating that the JNK pathway mediates growth inhibition and apoptosis of HSC.[23]

Finally, we determined whether ADSCs treated with bFGF could differentiate into hepatocytes. Western blot and RT-PCR analyses revealed that ADSCs treated with bFGF for 6 days did not show significant hepatocyte-specific marker expression compared with hepatocytes as the positive control (Fig. S1). These results suggest that addition of bFGF alone may be insufficient to induce hepatocyte differentiation.

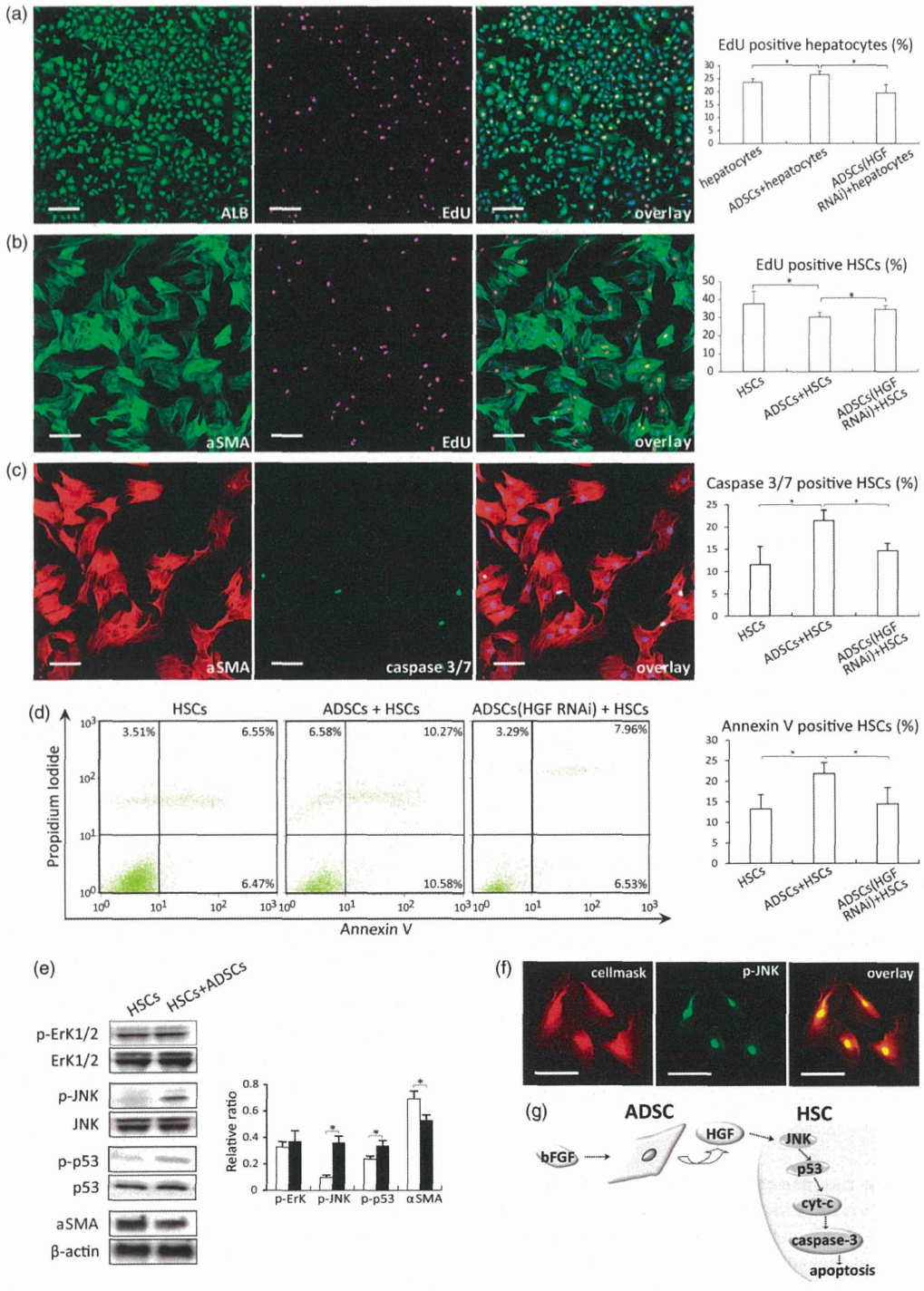

Figure 6 Apoptosis and proliferation of hepatocytes and HSCs in a co-culture model. The effect of adipose tissue-derived mesenchymal stem cells (ADSCs) on HSC and hepatocytes was analyzed after 3 days of co-culture. Representative images and quantitative analysis of EdU endocytosis by hepatocytes (a) and HSCs (b). The percentage of proliferating cells was calculated as EdU-positive nuclei/4′,6-diamidino-2-phenylindole positive nuclei × 100. (c) Representative images and quantitative analysis of caspase 3/7 activity in HSCs. (d) Representative plots of annexin V-PI double staining of HSCs. (e) HSCs were cultured with or without ADSCs. Western blot analyses of αSMA, phosphorylated Erk1/2, JNK, and p53. (f) Phosphorylation of JNK (green) in co-cultured HSCs was detected by immunofluorescence staining. Plasma membranes were stained using CellMask Deep Red plasma membrane stain (Invitrogen, Carlsbad, CA, USA). Scale bar = 20 μm. (g) Schematic model for the mechanism of JNK-p53 pathway involved in the induction of HSC apoptosis by ADSC. □, HSCs; ■, HSCs+ADSCs.

Discussion

Activated HSCs play a significant role in collagen and extracellular matrix (ECM) deposition that controls the development of liver fibrosis, and such excessive deposition of collagen and ECM was generally considered irreversible.[24,25] However, recent clinical studies found that liver cirrhotic patients who have been treated effectively demonstrate recovery with remodeling of fibrosis.[26] This finding indicates that it is feasible to augment the capacity for fibrotic tissue remodeling towards recovery. As a therapeutic approach, HGF is considered to be essential for tissue regeneration,[27,28] and HGF can be up-regulated by the microenvironment upon tissue damage.[29] In liver disease, HGF promotes HSC apoptosis, which is associated with its antifibrotic effect.[30] However, in neoplastic tissues, HGF functions as an antiapoptotic cytokine.[31,32] In the current study, ADSCs treated with bFGF showed significant up-regulation of HGF expression to physiologically relevant levels that enhanced the therapeutic effect on hepatic cirrhosis.

It appears reasonable that systemic ADSC infusion ameliorated liver injury, resulting in the histological and serological changes. To date, the mechanisms by which ADSCs exert their beneficial effects remain controversial. A previous study suggested that ADSCs exert their therapeutic effects on liver disease by either differentiating into functional hepatocyte-like cells or in a paracrine manner by secreting cytokines to promote repair.[16] However, the present study did not find obvious hepatic differentiation characteristics when ADSCs were treated with bFGF. In contrast, we found that bFGF promoted HGF expression in ADSCs, indicating that the therapeutic effects of bFGF-treated ADSCs on liver disease may be mediated in a paracrine manner. Our study also demonstrated that the infused ADSCs migrated into the liver and localized to the fibrosis area. Furthermore, double immunofluorescence revealed that the ADSCs expressed HGF efficiency *in vivo*. Moreover, co-culture experiments showed enhancement of hepatocyte proliferation but suppression of HSC survival by ADSCs, which could be responsible for the liver histological changes in ADSC-infused rats. In addition, the absence of HGF resulted in abrogation of the biological effects induced by ADSCs, which supports the notion that HGF secreted by ADSCs is important for the antifibrosis effect. Similarly, ADSCs accelerate tissue reperfusions in a limb ischemia model by secreting HGF, which also indicates HGF as an important factor for tissue repair.[33] In another study, activated HSCs showed increased nerve growth factor expression and induced apoptosis.[34] We found that HGF from ADSCs was involved in HSC apoptosis. These two distinct cytokines may cooperatively regulate apoptosis of HSCs. However, the contribution of other cytokines to HSC apoptosis remains unclear, and the potential involvement of other cells should be considered in future studies.

The JNK pathway is critical in mediation of HSC apoptosis.[35,36] Our data indicated the induction of JNK-p53-dependent apoptosis of HSC by ADSC. Together with the increased caspase-3/7 activity and the results from HGF RNA interference experiments, this study demonstrated that the overexpression of HGF induced HSC apoptosis via activation of JNK-p53 signaling, leading to the resolution of liver fibrosis.

Finally, compared with single infusion therapy, our work shows the first evidence that repeated administration of bFGF-treated ADSCs reduces hepatic injury and fibrosis formation more efficiently in animal model. Moreover, a potential therapeutic mechanism of ADSCs requires HGF production rather than engraftment. Previous work shows that ADSCs can be safe and highly efficient in clinical applications.[37] Our findings provide a rationale for the potential therapeutic application of ADSCs in patients with hepatic cirrhosis, suggesting that ADSC infusion could be a novel therapeutic approach for hepatic cirrhosis.

Acknowledgment

This work was financially supported by the Ministry of Education, Culture, Sports, Science, and Technology of Japan (KAKENHI no. 25462096).

References

1 Seki E, De Minicis S, Osterreicher CH *et al.* TLR4 enhances TGF-beta signaling and hepatic fibrosis. *Nat. Med.* 2007; **13**: 1324–32.
2 Hikita H, Takehara T, Kodama T *et al.* Delayed-onset caspase-dependent massive hepatocyte apoptosis upon Fas activation in Bak/Bax-deficient mice. *Hepatology* 2011; **54**: 240–51.
3 Iwaisako K, Brenner DA, Kisseleva T. What's new in liver fibrosis? The origin of myofibroblasts in liver fibrosis. *J. Gastroenterol. Hepatol.* 2012; **27**: 65–8.
4 Kakinuma S, Nakauchi H, Watanabe M. Hepatic stem/progenitor cells and stem-cell transplantation for the treatment of liver disease. *J. Gastroenterol.* 2009; **44**: 167–72.
5 Kiyohashi K, Kakinuma S, Kamiya A *et al.* Wnt5a signaling mediates biliary differentiation of fetal hepatic stem/progenitor cells in mice. *Hepatology* 2013; **57**: 2502–13.
6 Xu L, Gong Y, Wang B *et al.* Randomized trial of autologous bone marrow mesenchymal stem cells transplantation for hepatitis B virus cirrhosis: regulation of Treg/Th17 cells. *J. Gastroenterol. Hepatol.* 2014; **29**: 1620–8.
7 Kallis YN, Alison MR, Forbes SJ. Bone marrow stem cells and liver disease. *Gut* 2007; **56**: 716–24.
8 Gupta K, Hergrueter A, Owen CA. Adipose-derived stem cells weigh in as novel therapeutics for acute lung injury. *Stem Cell Res. Ther.* 2013; **4**: 19.
9 Zuk PA. The adipose-derived stem cell: looking back and looking ahead. *Mol. Biol. Cell* 2010; **21**: 1783–7.
10 Schäffler A, Büchler C. Concise review: adipose tissue-derived stromal cells—basic and clinical implications for novel cell-based therapies. *Stem Cells* 2007; **25**: 818–27.
11 Banas A, Teratani T, Yamamoto Y *et al.* Adipose tissue-derived mesenchymal stem cells as a source of human hepatocytes. *Hepatology* 2007; **46**: 219–28.
12 Dmitrieva RI, Minullina IR, Bilibina AA *et al.* Bone marrow- and subcutaneous adipose tissue-derived mesenchymal stem cells: differences and similarities. *Cell Cycle* 2012; **11**: 377–83.
13 McIntosh K, Zvonic S, Garrett S *et al.* The immunogenicity of human adipose-derived cells: temporal changes in vitro. *Stem Cells* 2006; **24**: 1246–53.
14 Puissant B, Barreau C, Bourin P *et al.* Immunomodulatory effect of human adipose tissue-derived adult stem cells: comparison with bone marrow mesenchymal stem cells. *Br. J. Haematol.* 2005; **129**: 118–29.
15 Banas A, Teratani T, Yamamoto Y *et al.* Rapid hepatic fate specification of adipose-derived stem cells and their therapeutic potential for liver failure. *J. Gastroenterol. Hepatol.* 2009; **24**: 70–7.
16 Gnecchi M, Zhang Z, Ni A, Dzau VJ. Paracrine mechanisms in adult stem cell signaling and therapy. *Circ. Res.* 2008; **103**: 1204–19.

17 Estes BT, Diekman BO, Gimble JM, Guilak F. Isolation of adipose-derived stem cells and their induction to a chondrogenic phenotype. *Nat. Protoc.* 2010; **1**: 1559–82.
18 Banas A, Teratani T, Yamamoto Y *et al.* In vivo therapeutic potential of human adipose tissue mesenchymal stem cells after transplantation into mice with liver injury. *Stem Cells* 2008; **26**: 2705–12.
19 Vinken M, Maes M, Oliveira AG *et al.* Primary hepatocytes and their cultures in liver apoptosis research. *Arch. Toxicol.* 2014; **88**: 199–212.
20 Trim JE, Samra SK, Arthur MJ *et al.* Upstream tissue inhibitor of metalloproteinases-1 (TIMP-1) element-1, a novel and essential regulatory DNA motif in the human TIMP-1 gene promoter, directly interacts with a 30-kDa nuclear protein. *J. Biol. Chem.* 2000; **275**: 6657–63.
21 Zaragosi LE, Ailhaud G, Dani C. Autocrine fibroblast growth factor 2 signaling is critical for self-renewal of human multipotent adipose-derived stem cells. *Stem Cells* 2006; **24**: 2412–19.
22 Kwon Y, Smith BD, Zhou Y *et al.* Effective inhibition of c-MET-mediated signaling, growth and migration of ovarian cancer cells is influenced by the ovarian tissue microenvironment. *Oncogene* 2015; **34**: 144–53. doi:10.1038/onc.2013.539
23 Kim WH, Matsumoto K, Nakamura T *et al.* Growth inhibition and apoptosis in liver myofibroblasts promoted by hepatocyte growth factor leads to resolution from liver cirrhosis. *Am. J. Pathol.* 2005; **166**: 1017–28.
24 Lin CL, Kao JH. Risk stratification for hepatitis B virus related hepatocellular carcinoma. *J. Gastroenterol. Hepatol.* 2013; **28**: 10–17.
25 Thabut D, Shah V. Intrahepatic angiogenesis and sinusoidal remodeling in chronic liver disease: new targets for the treatment of portal hypertension? *J. Hepatol.* 2010; **53**: 976–80.
26 Modi AA, Feld JJ, Park Y *et al.* Increased caffeine consumption is associated with reduced hepatic fibrosis. *Hepatology* 2010; **51**: 201–9.
27 Nakamura T, Sakai K, Matsumoto K. Hepatocyte growth factor twenty years on: much more than a growth factor. *J. Gastroenterol. Hepatol.* 2011; **26**: 188–202.
28 Flaquer M, Franquesa M, Vidal A *et al.* Hepatocyte growth factor gene therapy enhances infiltration of macrophages and may induce kidney repair in db/db mice as a model of diabetes. *Diabetologia* 2012; **55**: 2059–68.
29 Shiota G, Okano J, Kawasaki H *et al.* Serum hepatocyte growth factor levels in liver diseases: clinical implications. *Hepatology* 1995; **21**: 106–11.
30 Kodama T, Takehara T, Hikita H *et al.* Thrombocytopenia exacerbates cholestasis-induced liver fibrosis in mice. *Gastroenterology* 2010; **138**: 2487–98.
31 Zhu C, Ikemoto T, Utsunomiya T *et al.* Senescence-related genes possibly responsible for poor liver regeneration after hepatectomy in elderly patients. *J. Gastroenterol. Hepatol.* 2014; **29**: 1102–8.
32 Oyagi S, Hirose M, Kojima M *et al.* Therapeutic effect of transplanting HGF-treated bone marrow mesenchymal cells into CCl4-injured rats. *J. Hepatol.* 2006; **44**: 742–8.
33 Nakagami H, Maeda K, Morishita R *et al.* Novel autologous cell therapy in ischemic limb disease through growth factor secretion by cultured adipose tissue-derived stromal cells. *Arterioscler. Thromb. Vasc. Biol.* 2005; **25**: 2542–7.
34 Trim N, Morgan S, Evans M *et al.* Hepatic stellate cells express the low affinity nerve growth factor receptor p75 and undergo apoptosis in response to nerve growth factor stimulation. *Am. J. Pathol.* 2000; **156**: 1235–43.
35 Conner EA, Teramoto T, Wirth PJ *et al.* HGF-mediated apoptosis via p53/bax-independent pathway activating JNK1. *Carcinogenesis* 1999; **20**: 583–90.
36 Watson MR, Wallace K, Gieling RG *et al.* NF-kappaB is a critical regulator of the survival of rodent and human hepatic myofibroblasts. *J. Hepatol.* 2008; **48**: 589–97.
37 Parekkadan B, Milwid JM. Mesenchymal stem cells as therapeutics. *Annu. Rev. Biomed. Eng.* 2010; **12**: 87–117.

Supporting information

Additional Supporting Information may be found in the online version of this article at the publisher's web-site:

Figure S1 Western blot and RT-PCR Analysis of hepatocyte specific marker expression by cultured ADSC in the presence or absence of bFGF for 6 days. Representative results of five independent experiments with same findings.